# Strong coupling in molecular exciton-plasmon Au nanorod array systems

Stefano Fedele[1], Manal Hakami[1], Antony Murphy[2], Robert Pollard[2], James Rice[1]

[1]School of Physics, University College Dublin, Belfield, Dublin 4, Ireland.
[2]Centre for Nanostructured Media, The Queen's University of Belfast, Belfast BT7 1NN, UK

Keywords: Nanorod array, Excitons, porphyrins, strong coupling, reflection, photoluminescence, Raman

Corresponding author
James Rice,
School of Physics, University College Dublin,
Belfield, Dublin 4, Ireland.
Email: james.rice@ucd.ie
Phone: 00353 17172229

**Abstract**
We demonstrate here strong coupling between localized surface plasmon modes in self-standing nanorods with excitons in a molecular J-aggregate layer though angular tuning. The enhanced exciton−plasmon coupling creates a Fano like line shape in the differential reflection spectra associated with the formation of hybrid states, leading to anti-crossing of the upper and lower polaritons with a Rabi frequency of 125 meV. The recreation of a Fano like line shape was found in photoluminescence demonstrating changes in the emission spectral profile under strong coupling.

**Paper**
Developments in top-down and bottom-up nanofabrication techniques have enabled the development of active plasmonic nanomaterials such as arrays of gold nanorods with size- and shape-tunable plasmonic resonances [1-4]. Active plasmonics nanomaterials can be coupled with excitonic systems to give rise to hybrid plasmon–exciton modes (Plexcitons) when in the strong coupling regime [5-8]. Such systems when within the strong coupling limit effect changes in the optical processes of an emitter or absorber excitonic system. This offers potential to enhance or control exciton processes in excitonic systems such as organic semiconductors which offers opportunities for enhanced photonic device designs such as in light harvesting, optical sensing or artificial light sources [1,9,10]. An understanding of light mater interactions of plasmon-exciton complexes is central in fully realizing the potential of such complexes.

A number of studies have demonstrated plasmon-exciton in the strong coupling limit between an organic exciton semiconductor and a surface plasmons [11,12] and localized surface plasmons geometries [13-17]. Studies have demonstrated that colloidal Au nanoshell-J-aggregate particles exhibit strong coupling between the localized plasmons of a nanoshell and the excitons of molecular J-aggregates adsorbed on its surface [13]. The interaction of an organic exciton in a J-aggregate and surface plasmon polariton modes of nanostructured hole arrays or of nanosize metallic disks with different array periods was reported to exhibit strong coupling [14-16]. Tuning of plasmon–exciton coupling strength has been reported for strongly coupled exciton–plasmon states in Au nanodisk arrays coated with J-aggregate molecules achieved by changing the incident angle of incoming light, rather than changing the geometry

of the plasmonic nanomaterial. Using such an angle resolved approach plasmon–exciton coupling of variable strengths was achieved [17].

Strong coupling between plasmons on oriented gold nanorods arrays and J-aggregate molecular exciton has been demonstrated using a series of arrays with different architectures to control the spatial and spectral overlap between the plasmonic structure and exciton molecular aggregates [18]. Here we demonstrate tuning/detuning of strong coupling in self-standing nanorod arrays achieved though angular tuning. We report a Fano line shape in the differential reflection spectra associated with the formation of hybrid states, leading to anti-crossing of the upper and lower cavity-polaritons with a Rabi frequency of 125 meV. The recreation of a fano like line shape was also found in photoluminescence demonstrating changes in the emission spectral profile under strong coupling.

A schematic illustration of the sample i.e. a quasi-ordered free-standing Au nanorod arrays is shown in Figure 1(a). SEM studies (using a Jeol 6500F field emission SEM) reported that the Au nanorod substrate possesses a 70 ± 11 nm array period (center to center distance), a rod diameter 35 nm ± 7 and rod height of 200 ± 25 nm. The nanorods are encased in an anodic aluminum oxide (AAO) template which was removed prior to sample preparation via an etching solution in 30 mM NaOH as reported previously [3,4,18]. J-aggregate samples were prepared using meso-tetra (n-methyl-4-pyridyl) porphyrine tetra chloride (Frontier scientific) at pH=1 inducing J-aggregate formation by drop deposition as per reported procedures [19-21]. Reflection spectra from the nanorod array were measured in TE and TM polarizations and showed two broad bands associated with transverse and longitudinal modes from the nanorod array which are in line with literature reports (as shown in Figure 1(b)) [3,4,18]. Reflection spectra were recorded for the J-aggregate/nanorod sample as a function of ($\Delta R/R = (R_{sample} - R_{background})/R_{background}$) using a gold mirror background reference. A optical extinction spectrum (e.g. shown as $-\Delta R/R$) of a gold nanorod sample recorded is shown in Figure 1(b) showing the presence of transverse modes and longitudinal modes of the nanorod. Optical extinction spectroscopy of the porphyrin in monomeric form was recorded along with the porphyrin in J-aggregate form as shown in Figure 1(b). The J-aggregate spectrum shows B (Soret or $S_2$ exciton state) bands at 425 and 495 nm [19]. The spectrum shows also a Q-band ($S_1$ exciton state) region with a strong peak at 675 nm. The redistribution of B and Q intensities following aggregation been attributed to intensity transfer from the B- to the Q-band region that is mediated by an excitonic coupling between B and Q transition dipoles.

Raman and fluorescence measurements were performed at ambient temperature using a custom-built, open-bench Raman system in epi-fluorescence backscattering configuration with 532, 473 and 633 nm excitation [22-25] with the laser focused to a spot size of c.a. 10 μm. The emission from the J-aggregate/nanorod complex is shown in Figure 1(c). The photoluminescence (PL) intensity for the J-aggregate/nanorod complex is reduced (quenched) compared to the J-aggregate on the dielectric glass. Fluorescence lifetime measurements where recorded showing a reduction in the radiative lifetime (from 2.3 to 1.6 ns for the J-aggregate/nanorod sample compared to J-aggregate/glass). A change in the PL intensity and the spontaneous emission rate can potentially be attributed to the Purcell effect due to the local SP field, suggesting weak coupling and/or to charge transfer of the exciton to the metal resulting in enhanced non-radiative pathways for the J-aggregate [8]. However, similar observations can occur in the strong coupling limit also. Raman spectroscopy of the porphyrin and J-aggregate samples on a gold nanorod substrate or glass are shown in Figure 1(d). Raman spectroscopy was performed at 532 nm in resonance with the Q band of both the J-aggregate and monomeric porphyrin resulting in resonance enhancement in addition to plasmonic enhancement. The Raman spectrum recorded on the nanorod

substrate enhances the Raman signal strength. The origin of the increased signal intensity is assigned to plasmonic resonance Raman enhancement (known also as surface enhanced resonance Raman or SERRS).

Reflection measurements in un-polarized and TE and TM polarized light for the J-aggregate/nanorod system were undertaken. Figure 2(a) shows a series of three spectra taken at a single incident angle (θ=degree) corresponding to three different polarizations. In line with previous studies literature polarized reflection spectra showed that TE polarized SP modes are at lower energy (red-shifted) compared to TM polarized SP modes which are located at a higher energy due to a stronger restoring force of the charge oscillation [27]. Figure 2(b) shows the differential reflectance (ΔR/R) from the J-aggregate nanorod sample for TM polarized light at three different indecent angles. The three differential reflectance spectra show broad dips centered around 475 and 675 nm, with the specific features at these regions dependent upon angle of incident. The dips in the reflection spectra are related to backscattering from SP associated with transversal and longitudinal modes of the nanorod array. Concentrating on the wavelength range nm 600-750 nm which corresponds to a spectral region where the J-aggregate $S_1$ exciton state absorbs and also where the nanorods longitudinal SP mode is present. To assess how the reflection spectra depends upon angle a more detailed series of measurements were undertaken with a consecutive series of reflection spectra recorded at incident angles from 20 to 80 degrees recorded at every 2.5 degree interval. Figure 2(c and d) shows the TM differential reflection spectra. The spectra show at θ = 35 degrees a strong dip at c.a. 645 nm, as the angle increases this dip decreases in intensity and a dip at c.a. 705 nm emerges and grows in intensity as the angle increases. This is seen clearly in the contour plot (Figure 2(d)) which shows that there is a clear dip coinciding with the exciton energy replicating a fano resonance line-shape which indicates the presence of strong coupling. As schematically outlined in Figure 1(e) (and based on Salomon et al [16]) in the strong coupling regime plexcitons are formed from interaction of the $|S_1>$ state of the exciton molecular J-aggregate with the longitudinal ($|SP_L>$) surface plasmon modes of the gold nanorod array. The hybrid plexcitons possessing two branches (e.g. $|S_1\text{-}SP_L>^+$ and $|S_1\text{-}SP_L>^-$). The reflection spectrum shows two dips marked $|S_1\text{-}SP_L>^+$ and $|S_1\text{-}SP_L>^-$ at 645 nm and 700 nm respectively (which corresponds to Rabi splitting (Ω) energy of 150 meV). Figure 2 (c) and (Figure 2(d)-insert) shows the $S_1$ Q band from the J-aggregates absorption spectrum which has a peak at 675 nm which is c.a midway between the $|S_1\text{-}SP_L>^+$ and $|S_1\text{-}SP_L>^-$ hybrid states. To confirm the presence of strong coupling a dispersion plot was made. A dispersion plot (Figure 2(d)) as a function of the single longitudinal SP mode of pristine nanorod with the Plexciton hybrid modes of the J-aggregate/nanorod complex with incident angle is shown in Figure 2(e). The dispersion plot shows a characteristic anti-crossing of the two hybrid peaks ($|S_1\text{-}SP_L>^+$ and $|S_1\text{-}SP_L>^-$). This is associated with Rabi splitting of the SP peak, where the molecular resonance of the J-aggregate and the longitude mode of the nanorod array overlap characteristic of the strong coupling. `

The PL from the J-aggregate-nanorod complex was generated by tuning the excitation wavelength (at 632 nm) towards been in resonant with the Q band of the J-aggregate centered at 675 nm arising form $^{1,3}E_1 \leftarrow {}^{1,3}E_3$ with inter-porphyrin charge resonance transitions. Figure 3(a and c) shows the fluorescence spectra recorded as a function of incident angle. The main peak in the florescence spectra shifts progressively to the blue e.g. c.a. 730 (θ=0) to 725 (θ=20) to 682 (θ=40) to 674 (θ=60) nm. This shift in position can be seen more clearly by subtraction of the J-aggregate emission (θ=0) on glass from that of J-aggregate/nanorod at each angle (shown in Figure 3(b)). Following subtraction the spectra show a dip at 715 nm, this dip corresponds to the position of the maximum band position from the reference J-

aggregate fluorescence spectrum recorded on a dielectric (glass) medium. Similar spectral profiles have been reported for PL from systems in the strong-coupling limit [12,27]. Spectrally modified plasmon enhanced fluorescence or plasmon fluorescence quenching has been reported for molecular systems coupled with plasmonic structures [28]. Such studies reported that the modification in the fluorescence profile is associated with the spectral dependence of the radiative and non-radiative decay rate of the molecular exciton complex closely follows the plasmon scattering spectrum. Figure 3(b) shows that the PL spectral profile moves to the blue with increasing incident excitation angle which follows the observed shift in the reflection measurements (Figure 2). This indicates that the PL arises from the polaritonic emission, resulting from the Plexciton SP/exciton mixed states.

Recently it has been demonstrated that SP modes play a significant role in the observed Raman background in SERS [29]. The authors reporting that the background in SERS comes from contributions centred strongest at the plasmon resonance regions in systems with localised SP modes such as in Au nanorod arrays. The SP modes provide the strongest out-coupling of the radiation from the electrons relaxing back down from the virtual inelastic light scattering state. The spectral resonance of the plasmons thus dictates which energy range of electrons contributes to the Raman (Stokes) background. SERRS spectroscopy was performed to assess the impact of angle. Figure 3(a)-insert shows SERS spectra recorded at 532 nm. A base line formation routine (Origin Labs) to highlight the background on which the spectra are located was used to assess the contribution of the background in regard to the spectral profile. The resulting spectra show that there is a change in the background profile. Looking at the background it can be seen that the background shifts to the blue with increasing angle similar to that seen for the PL spectra.

In summary, we demonstrate here strong coupling between localised surface plasmon modes in self-standing nanorods with Frankel excitons in a porphyrin molecular J-aggregate layer though angle tuning. The enhanced exciton−plasmon coupling creating a Fano line shape in the differential reflection spectra associated with the formation of plexciton hybrid states, leading to anti-crossing of the upper and lower cavity-polaritons with a Rabi frequency of 125 meV. The recreation of a fano like line shape was found in photoluminescence demonstrating changes in the emission spectral profile under strong coupling. This study demonstrates that J-aggregate excitons under strong coupling with plasmon modes can controllable alter the emission and absorption spectral profile through control of excitation angle.

Acknowledgement

The UCD Nanophotonics and Nanoscopy Research Group is supported by Science Foundation Ireland grant 12/IP/1556. The Centre for Nanostructured Media acknowledges the Engineering and Physical Sciences Research Council (EPSRC - UK) for financial support (Grants EP/H000917, EP/I014004).

References

1. Active Plasmonics and Tuneable Plasmonic Metamaterials. Anatoly V. Zayats, Stefan Maier (Editor). Wiley, 2013.

2. Kabashin, A. V., P. Evans, S. Pastkovsky, W. Hendren, G. A. Wurtz, R. Atkinson, R. Pollard, V. A. Podolskiy, and A. V. Zayats. Nat. Material **8**, 867 - 871 (2009)

3. Damm, S., Fedele, S., Murphy, A., Holsgrove, K., Arredondo, M., Pollard, R., and J.H. Rice. Appl. Phys. Lett. **106**, 183109 (2015).

4. Damm, S., Lordan, F., Murphy, A., McMillen, M., Pollard, R. and J. H. Rice. Plasmonics, **9**, 1371-1376 (2014).

5. Barnes, W. L., Dereux, A., and T. W. Ebbesen, Nature **424**, 824 (2003).

6. Koenderink, A. F., Alù, A., and A. Polman. Science **348**, 516 (2015).

7. Novotny, L. Am. J. Phys. **78**, 1199 (2010)

8. Purcell, E. M. Phys. Rev. **69**, 37 (1946).

9. Gonzalez-Ballestero, C., Feist, J. Moreno E. and F.J. Garcia-Vidal. Phys. Rev. B. **92**, 121402(R) (2015)

10. Zhao, J., Sherry, L .J., Schatz, G. C., and R. P. Van Duyne. IEEE J. Quant. Electron., **14**, 1418 (2008)

11. Bellessa, J., Bonnand, C., Plenet, J.C. and J. Mugnier. Phys. Rev. Lett, **93**, 036404 (2004).

12. Symonds, C., Bellessa, J., Plenet, J.C., Bréhier, A., Parashkov, R., Lauret, J.S. and E. Deleporte. Appl. Phys. Lett., **90**, 091107 (2007).

13. Fofang, N.T., Park, T.H., Neumann, O., Mirin, N.A., Nordlander, P. and N. J. Halas. Nano Lett., **8**, 3481–3487 (2008).

14. Dintinger, J., Klein, S., Bustos, F., Barnes, W.L., and T. W. Ebbesen,. Phys. Rev. B, **71**, 035424 (2005).

15. Bellessa, J., Symonds, C., Vynck, K., Lemaitre, A., Brioude, A., Beaur, L. Plenet, J.C., Viste, P., Felbacq, D. and E. Cambril. Phys. Rev. B, **80**, 033303 (2009).

16. Salomon, A., Wang, S., Hutchison, J. A., Genet, C. and Ebbesen, T. W. ChemPhysChem, **14**, 1882-1886 (2013).

17. Zheng, Y. B., Juluri, B. K., Lin Jensen, L., Ahmed, D., Lu, M., Jensen, L. and Huang, T. J. Adv. Material, **22**, 3603-3607 (2010).

18. Wurtz, G. A., Evans, P. R., Hendren, W., Atkinson, R., Dickson, W., Pollard, R. J. and C. Bower,. Nano Lett. **7**, 1297–1303 (2007).

19. Reddy, M.H., Al-Shammaria, R., Al-Attar, N., Lopez, S., Keyes, T. and J. H. Rice. Mat. Res. Express, **1**, 045038 (2014).

20. Reddy, H. V., Al-Shammaria, R. M., Al-Attara, N., Kennedy, E., Rogers, L., Lopezc, S., Keyes, T. E., Senge, M. O. and J. H. Rice. Phys. Chem. Chem. Phys.,**16**, 4386-4393 (2014).

21. Reddy, M. H. V., Al-Shammari, R. M., Al-Attar, N., Rogers, L., Lopez, S., Forster, R. J. and J. H. Rice. Chem. Phys. Materials. **143**, 963-968 (2014).

22. Lordan, F. Rice, J. H., Jose, B., Forster, R. J., Keyes T.E. J. Phys. Chem. C **116**, 1784-1788 (2012)

23. Damm, S., Carville, N. C., Rodriguez, B. J., Manzo, M., Gallo, K. and J. H. Rice. J. Phys. Chem. C **116**, 26543-26550 (2012)

24. Al-Attar, N., Kopf, I., Kennedy, E., Flavin, K., Giordani, S. and J. H. Rice, Chem. Phys. Lett. **535**, 146-151 (2012)

25. Damm, S., Carville, N. C., Manzo, M., Gallo, K., Lopez, S. G., Keyes, T. E. and J. H. Rice. Appl. Phys. Lett. **103**, 083105 (2013)

26. Najmaei, S., Mlayah, A., Arbouet, A., Girard, C., Léotin, J. and J. Lou. ACS nano, **8**, 12682-12689 (2014).

27. Lee, B., Park, J., Han, G. H., Ee, H. S., Naylor, C. H., Liu, W. and R. Agarwal, R. "Fano resonance and spectrally modified photoluminescence enhancement in monolayer MoS2 integrated with plasmonic nanoantenna array Nano letters on line pre publication (2015).

28.Le Ru, E. C., Etchegoin, P. G., Grand, J., Felidj, N., Aubard, J. and G. Levi. J. Phys. Chem. C, **111**, 16076-16079 (2007).

29. Hugall, J. T. and J J. Baumberg. Nano letters, **15**, 2600-2604 (2015).

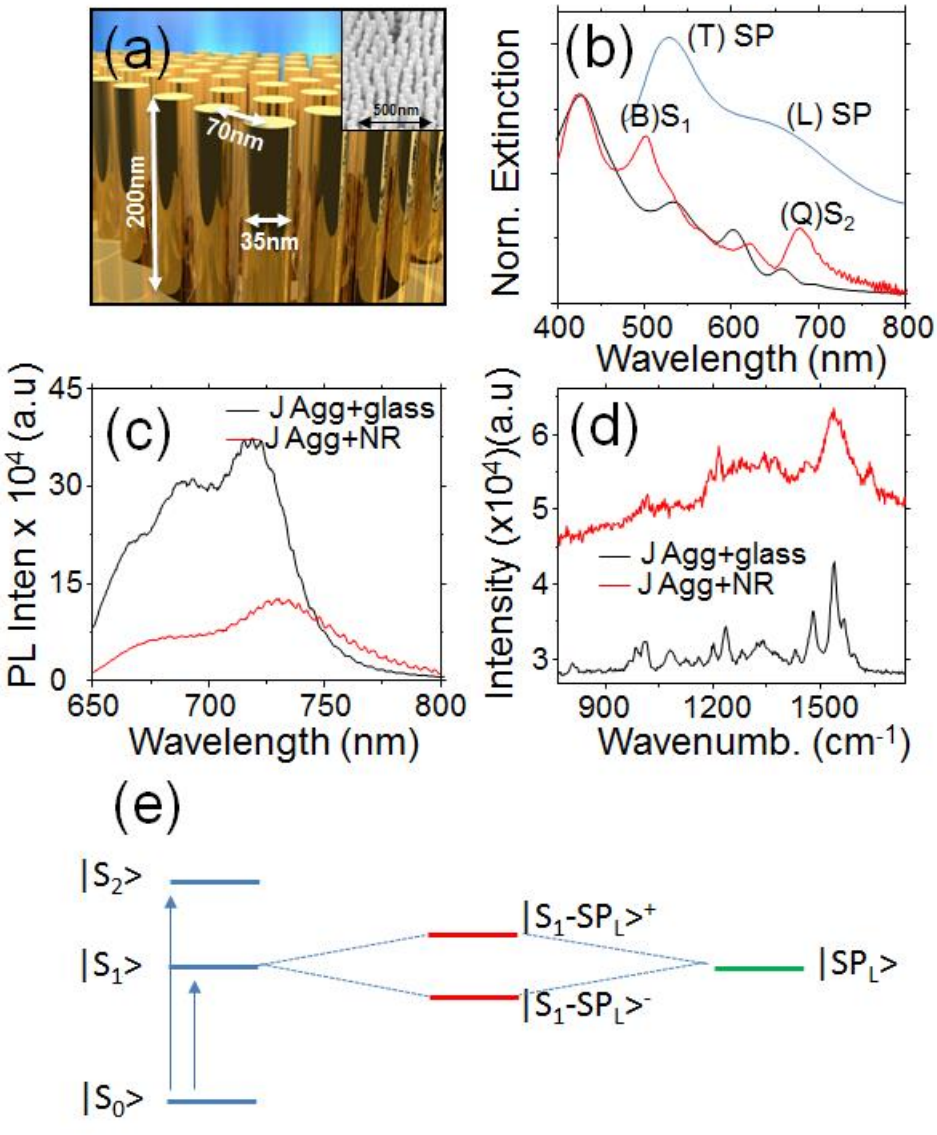


Figure 1. (a) Schematic drawing of the nanorod array. (b) Extinction spectra of a J-aggregate thin film on glass (red) shown along with a thin film of the initial monomer porphyrin (black) recorded using optical absorption spectroscopy, shown also is a spectrum for the nanorod sample (blue) recorded using optical reflection spectroscopy, shown as the inverse of ΔR/R. (c) Fluorescence spectroscopy of J-aggregate on a gold nanorod substrate (J-Agg+NR) and on glass (J-Agg+glass) samples recorded at 470 nm in resonance with the J-aggregate B band. (d) Raman spectroscopy of J-aggregate on a gold nanorod substrate (J-Agg+NR) and on glass (Por+glass) recorded at 532 nm. (e) Schematic drawing of the electronic states for a strong coupling scheme showing the Plexciton states.

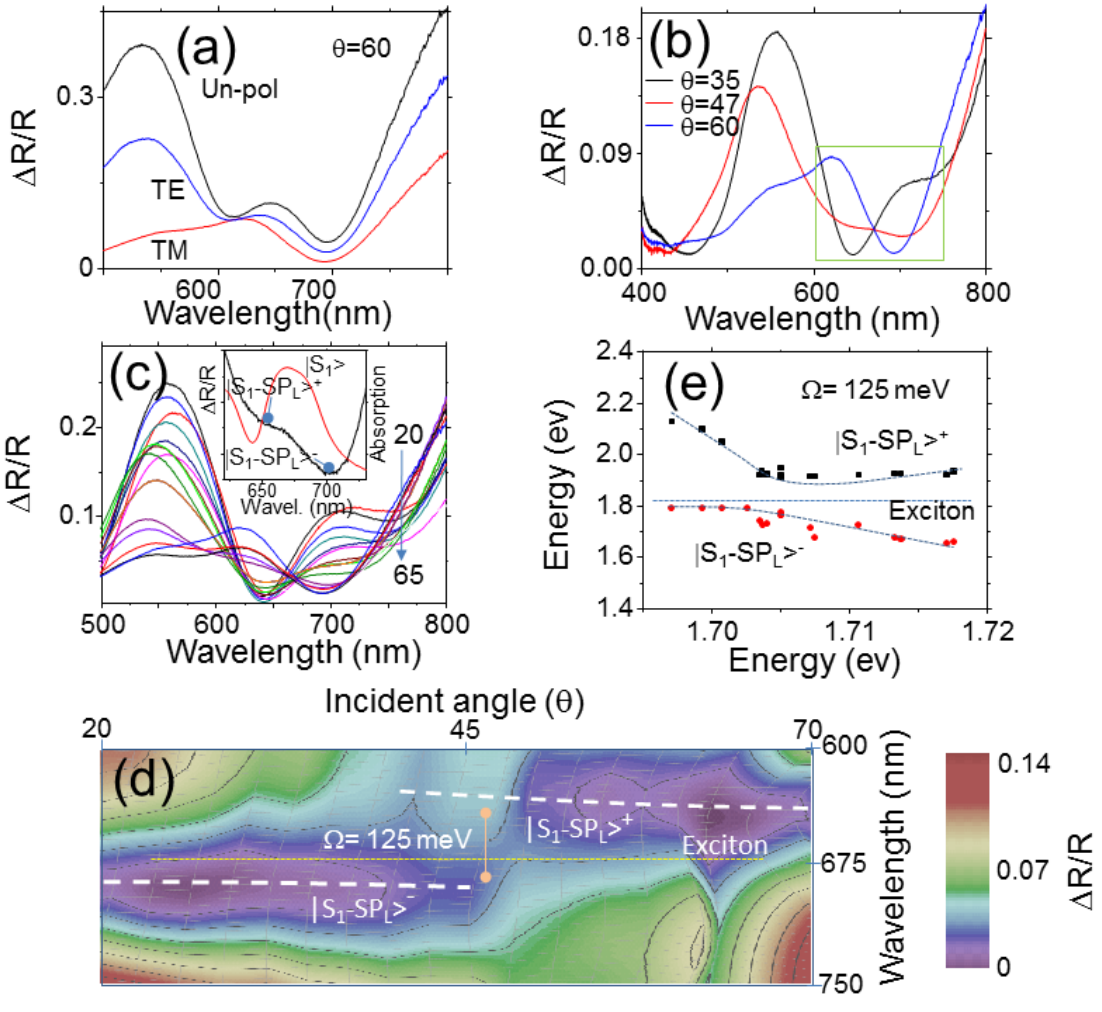


Figure 2. Polarized reflection spectra for J-aggregate on a gold nanorod substrate. (a) Three TM spectra recorded at three different angles of incidence corresponding to the region of the nanorods SP modes and also of the exciton absorption of the J-aggregate. (b) Three spectra were recorded over a range of angles with respect of the incidence angle. Inset shows TM, TE and unpolarized differential reflection spectra (c) Spectral plot and contour plot (d) of the TM polarized reflection spectra at different incident angles. The spectra were recorded between 600 and 750 nm corresponding to the nanorods longitudinal SP mode and also of the $S_1$ absorption of the J-aggregate. Insert shows a single reflection spectrum from the J-aggregate-nanorod complex (recorded at 47 degrees) along with the optical absorption spectrum of the J-aggregate. (e) Dispersion curve of plexciton hybrid bands as a function of bare nanorod longitude SP position.

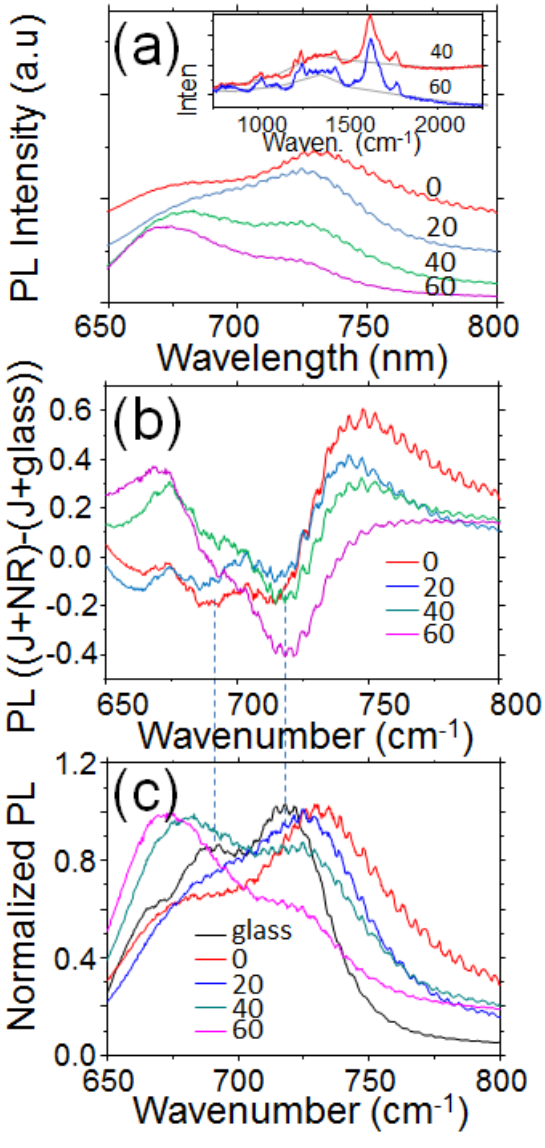


Figure 3. PL spectroscopy of the J-aggregate on a gold nanorod substrate $\lambda_{ex}$ = 632 nm. (a) PL spectra recorded at four different excitation angles. Insert shows SERS of the J-aggregate/nanorod complex for angles of excitation at 40 and 60 degrees. $\lambda_{ex}$ = 532 nm. These angles are above and below the critical angle of .c.a. 47 degrees where the hybrid mode splits. (b) Subtraction of J-aggregate on a gold nanorod substrate spectra recorded at each of the four excitation angles shown in (a) from J-aggregate on a dielectric glass substrate. (c) Normalized overlaid PL spectra recorded from J-aggregate on a gold nanorod substrate recorded at each of the four excitation angles and J-aggregate on a dielectric glass substrate.